

# Binding of Different Divalent Cations to the Active Site of Avian Sarcoma Virus Integrase and Their Effects on Enzymatic Activity\*

(Received for publication, March 4, 1997, and in revised form, April 22, 1997)

Grzegorz Bujacz<sup>‡§</sup>, Jerry Alexandratos<sup>‡</sup>, and Alexander Wlodawer<sup>‡¶</sup>

From the <sup>‡</sup>Macromolecular Structure Laboratory, NCI-Frederick Cancer Research and Development Center, ABL-Basic Research Program, Frederick, Maryland 21702, and the <sup>§</sup>Faculty of Food Chemistry and Biotechnology, Technical University of Łódź, Łódź, Poland

George Merkel, Mark Andrade, Richard A. Katz, and Anna Marie Skalka

From the Institute for Cancer Research, Fox Chase Cancer Center, Philadelphia, Pennsylvania 19111

Retroviral integrases (INs) contain two known metal binding domains. The N-terminal domain includes a zinc finger motif and has been shown to bind  $Zn^{2+}$ , whereas the central catalytic core domain includes a triad of acidic amino acids that bind  $Mn^{2+}$  or  $Mg^{2+}$ , the metal cofactors required for enzymatic activity. The integration reaction occurs in two distinct steps; the first is a specific endonucleolytic cleavage step called “processing,” and the second is a polynucleotide transfer or “joining” step. Our previous results showed that the metal preference for *in vitro* activity of avian sarcoma virus IN is  $Mn^{2+} > Mg^{2+}$  and that a single cation of either metal is coordinated by two of the three critical active site residues (Asp-64 and Asp-121) in crystals of the isolated catalytic domain. Here, we report that  $Ca^{2+}$ ,  $Zn^{2+}$ , and  $Cd^{2+}$  can also bind in the active site of the catalytic domain. Furthermore, two zinc and cadmium cations are bound at the active site, with all three residues of the active site triad (Asp-64, Asp-121, and Glu-157) contributing to their coordination. These results are consistent with a two-metal mechanism for catalysis by retroviral integrases. We also show that  $Zn^{2+}$  can serve as a cofactor for the endonucleolytic reactions catalyzed by either the full-length protein, a derivative lacking the N-terminal domain, or the isolated catalytic domain of avian sarcoma virus IN. However, polynucleotidyl transferase activities are severely impaired or undetectable in the presence of  $Zn^{2+}$ . Thus, although the processing and joining steps of integrase employ a similar mechanism and the same active site triad, they can be clearly distinguished by their metal preferences.

is an important target for the design of drugs that block the replication of pathogenic retroviruses such as the human immunodeficiency virus (HIV). The integration reaction occurs in two distinct steps. First, IN nicks the viral DNA near the 3'-ends of both strands (the “processing” reaction); it then inserts these ends into host target DNA (the joining reaction). Both reactions comprise a nucleophilic attack by a hydroxyl oxygen on a phosphorous atom in the DNA backbone; the hydroxyl is derived from a water molecule in the processing reaction and from the newly formed 3'-OH at the end of the viral DNA in the joining reaction. Divalent cations  $Mn^{2+}$  or  $Mg^{2+}$  are known to be required as cofactors. *In vitro* the reactions are most efficient in the presence of  $Mn^{2+}$ , but as  $Mg^{2+}$  is more abundant in living cells, it is generally presumed to be the physiologically relevant cation.

Retroviral integrases contain approximately 300 amino acids and are composed of three domains (4). The first two domains are highly conserved, and both include metal-binding sites. The N-terminal domain (amino acids ~1–50) contains a zinc finger-like motif, HHCC. Binding of  $Zn^{2+}$  at this site stabilizes the structure of HIV-1 IN and enhances multimerization and activity (5–7). The central, catalytic domain (amino acids ~50–200) is characterized by a triad of invariant acidic amino acids (Asp-64, Asp-121, and Glu-157 in ASV IN), the last two separated by 35 amino acids comprising the D,D(35)E motif. These three acidic residues are essential for both processing and joining activity and have been proposed to bind the divalent metal cofactors during catalysis (8).

Solution of the crystal structures of the isolated catalytic core domains of HIV-1 (9, 10) and ASV IN (11, 12) have revealed that these retroviral enzymes belong to a superfamily of nucleases and polynucleotidyltransferases, all of which contain a cluster of conserved acidic amino acids at their presumed active sites. HIV-1 reverse transcriptase ribonuclease H (RNase H) domain, another member of this superfamily, was shown to bind two divalent cations in this site (13), prompting the suggestion (14) that all members of this family may use a two-metal catalytic mechanism like that deduced for the 3'-5' exonuclease of *Escherichia coli* DNA polymerase I (15, 16). We have shown that side chains of two of the acidic triad residues in the D,D(35)E motif in ASV IN also form a metal binding pocket. A single ion,  $Mn^{2+}$  or  $Mg^{2+}$ , is complexed to Asp-64 and Asp-121 when crystals of the isolated catalytic domain of ASV IN are soaked in metal-containing solutions (12). We hypothesized that a second metal might be bound between the Asp-64 and Glu-157 in the full-length protein or in the presence of substrate.

The retroviral integrase (IN)<sup>1</sup> is a virus-encoded enzyme that catalyzes integration of viral DNA into host DNA (1–3). As DNA integration is an essential step in the virus life cycle, IN

\* The work was supported in part by the NCI, DHHS, National Institutes of Health. Other support includes National Institutes of Health Grants CA-47486 and CA-06927, a grant for infectious disease research from Bristol-Myers Squibb Foundation, and an appropriation from the Commonwealth of Pennsylvania. The costs of publication of this article were defrayed in part by the payment of page charges. This article must therefore be hereby marked “advertisement” in accordance with 18 U.S.C. Section 1734 solely to indicate this fact.

The atomic coordinates and structure factors (codes IVSI, IVSH, and IVSJ) have been deposited with the Protein Data Bank, Brookhaven National Laboratory, Upton, NY.

¶ To whom correspondence should be addressed. Tel.: 301-846-5036; Fax: 301-846-6128; E-mail: wlodawer@ncifcrf.gov.

<sup>1</sup> The abbreviations used are: IN, integrase; HIV, human immunodeficiency virus; ASV, avian sarcoma virus.

TABLE I  
Structural data for ASV IN complexed with different divalent cations

Crystals were soaked in metal salts at the indicated concentrations. Maximum resolution of the diffraction data is given for each data set. Metals bind to the residues in up to four sites, as noted. Peak heights are given in the root mean square units of map density, whereas *B*-factors are in Å<sup>2</sup>. All occupancies are considered to be full unless otherwise noted (in parentheses). See text for the discussion of partial occupancies.

Metal	Resolution	<i>R</i> -factor	Site I ASP-64–Asp-121 peak height/ <i>B</i> -factor (occupancy)	Site II Asp-64–Glu-157 peak height/ <i>B</i> -factor (occupancy)	Site III His-103 peak height/ <i>B</i> -factor (occupancy)	Site IV His-198–Tyr-194 peak height/ <i>B</i> factor (occupancy)
	Å					
Mg <sup>2+</sup> (500 mM)	1.75	0.150	13.3/20.1	—	—	—
Mg <sup>2+</sup> (100 mM)	1.81	0.137	13.6/20.0	—	—	—
Mg <sup>2+</sup> (20 mM)	2.20	0.138	5.8/NA <sup>a</sup>	—	—	—
Mn <sup>2+</sup> (500 mM)	2.5	0.178	9.9/ND <sup>b</sup>	—	—	—
Mn <sup>2+</sup> (100 mM)	2.0	0.179	14.3/25.5	—	—	—
Mn <sup>2+</sup> (10 mM)	2.05	0.130	16.8/30.8	—	—	—
Ca <sup>2+</sup> (100 mM)	2.2	0.173	11.2/41.8	—	—	—
Cd <sup>2+</sup> (100 mM)	2.0	0.175	22.5/22.5	9.37/34.8 (0.45)	—	—
Zn <sup>2+</sup> (2 mM)	2.0	0.174	10.9/31.7 (0.6 )	7.3/49.9 (0.3 )	6.4/55.0 (0.2)	14.9/31.0
Mg <sup>2+</sup> + Zn <sup>2+</sup> (100 mM each)	2.2	0.177	13.7/28.1 Zn <sup>2+</sup>	13.6/41.0 Zn <sup>2+</sup>	10.2/54.7 Zn <sup>2+</sup>	5.2/70.3 Zn <sup>2+</sup>
Mn <sup>2+</sup> + Zn <sup>2+</sup> (100 mM each)	2.2	0.166	13.4/32.6 Zn <sup>2+</sup>	9.8/50.5 Zn <sup>2+</sup>	9.0/46.6 Zn <sup>2+</sup>	6.0/73.1 Zn <sup>2+</sup>
Mn <sup>2+</sup> + Zn <sup>2+</sup> (10 mM each)	2.0	0.183	12.5/35.4 (0.33) Zn <sup>2+</sup>	7.4/35.6 (0.33) Zn <sup>2+</sup>	8.2/60.2 (0.5) Zn <sup>2+</sup>	12.5/24.8 Zn <sup>2+</sup>
			12.5/23.0 (0.67) Mn <sup>2+</sup>			

<sup>a</sup> Not applicable.

<sup>b</sup> Not determined.

Here we show that additional divalent cations can also bind in the active site of crystals of the isolated catalytic core domain of ASV IN. Moreover, in the case of Zn<sup>2+</sup> and Cd<sup>2+</sup>, two ions are complexed by side chains from all three of the acidic amino acids of the D,D(35)E motif. To investigate the significance of these observations, we measured enzymatic properties in the presence of these metals with the isolated catalytic core, full-length ASV IN protein and an N-terminal deletion derivative that lacks the zinc finger motif but retains both processing and joining activities. The results of the structural analysis are consistent with a two-metal reaction mechanism. The biochemical studies show that whereas Zn<sup>2+</sup> is a cofactor for the hydrolytic, nicking activities, it provides little or no detectable support for the polynucleotidyltransferase activities of IN.

#### MATERIALS AND METHODS

**Crystallographic Procedures**—Expression, purification, and crystallization of the catalytic core domain of ASV IN have been described previously (11), and the crystals used here were grown by the same procedures. Salts of divalent cations used in this study were dissolved in the well buffer to produce the soaking solutions. The crystals were soaked for 2–3 days, as in the previous studies (12). Some experiments were performed on crystals grown directly in the presence of divalent cations without finding any difference in their mode of binding (data not shown).

Diffraction data were collected at room temperature on MAR300 or DIP2020 image plate detectors using graphite-monochromated CuK<sub>α</sub> radiation. They were processed with DENZO and scaled with SCALEPACK (17). Data with  $F > 2\sigma(F)$  were used in refinement, and the low resolution cutoff was either 8 or 10 Å. Structure refinements were carried out using the program PROLSQ (18), which was modified to utilize free *R*-factor computation. Some structures were refined with 8% of the separately and randomly chosen data reserved for that purpose, whereas other refinements did not utilize free *R*-factor (see Table I). Structures of the Mn<sup>2+</sup> and Mg<sup>2+</sup> complexes were refined very carefully until final convergence, whereas other structures were modeled carefully only in the vicinity of the metal-binding sites, with other areas subject to less careful rebuilding. This is reflected in somewhat higher *R*-factors for these structures, which are nevertheless adequate to impart confidence in the structural results described here. The coordinates of the complexes with Ca<sup>2+</sup>, Zn<sup>2+</sup>, and Cd<sup>2+</sup> have been deposited with the Protein Data Bank, Brookhaven National Laboratory, Upton, NY (accession codes 1VSI, 1VSH, and 1VSJ, respectively). The coordinates of selected Mg<sup>2+</sup> and Mn<sup>2+</sup> complexes were deposited previously (12).

**Processing, Nicking, and Disintegration Assays**—The full-length

ASV IN and the catalytic IN-(39–286) were purified as described previously (19). Assays were carried out exactly as described (11). Briefly, for nicking and processing, the substrate was an 18-base pair duplex corresponding to the U3 end of ASV DNA. The 5'-end of the plus strand was labeled with <sup>32</sup>P. The reaction mix contained 50 mM Tris, pH 8.4, 2 mM β-mercaptoethanol, 200 μg/ml bovine serum albumin, 50 mM NaCl, and 4% glycerol. Reactions were carried out in substrate excess. For processing and joining, the concentration of IN was 2 μM, and the DNA substrate was 15 μM. For disintegration reactions, the concentration of IN was 1 μM, and the DNA substrate was 8 μM. The disintegration substrate was prepared by annealing four separate DNA strands of 19, 16, 10, and 9 nucleotides with the 10-nucleotide strand end-labeled with <sup>32</sup>P. Reactions were carried out at the indicated times and metal concentrations. Reaction products were fractionated on 20% acrylamide-urea sequencing gels, and bands were quantified using a Fuji phosphorimager. Results are expressed as μmol of product/μmol of IN monomer or IN fragment.

#### RESULTS

**Mn<sup>2+</sup>, Mg<sup>2+</sup>, and Ca<sup>2+</sup> Bind to a Single Site in ASV Catalytic Domain**—In our earlier studies, we soaked crystals of the isolated ASV IN catalytic domain with the two known divalent cation cofactors, Mn<sup>2+</sup> and Mg<sup>2+</sup> (12). We observed coordination of both cations between Asp-64 and Asp-121 of the catalytic triad but no participation of its third member, Glu-157. To further investigate the possible participation of Glu-157 in metal binding, we carried out a systematic analysis encompassing a variety of divalent cations and a wider range of concentrations.

Crystals of the catalytic domain of ASV IN-(52–207) were soaked in 2–500 mM solutions of five divalent cations: Mg<sup>2+</sup>, Mn<sup>2+</sup>, Zn<sup>2+</sup>, Ca<sup>2+</sup>, and Cd<sup>2+</sup>. Structures of the metal-soaked crystals were solved and refined at moderately high resolution (Table I). As reported earlier, the electron density map corresponding to the structure of the Mg<sup>2+</sup> complex obtained at the highest concentration of its salt is exceptionally clear and shows a cation bound between the carboxylates of Asp-64 and Asp-121 of the D,D(35)E motif (denoted site I). However, no indication of binding of a second cation could be found in this map. Less than 30% occupancy was observed at a lower concentration of Mg<sup>2+</sup> (20 mM), indicating that binding was much weaker. A putative metal/water cluster did not refine well. However, a similarly positioned, single metal ion was detected at full occupancy after soaking the crystals in an even lower

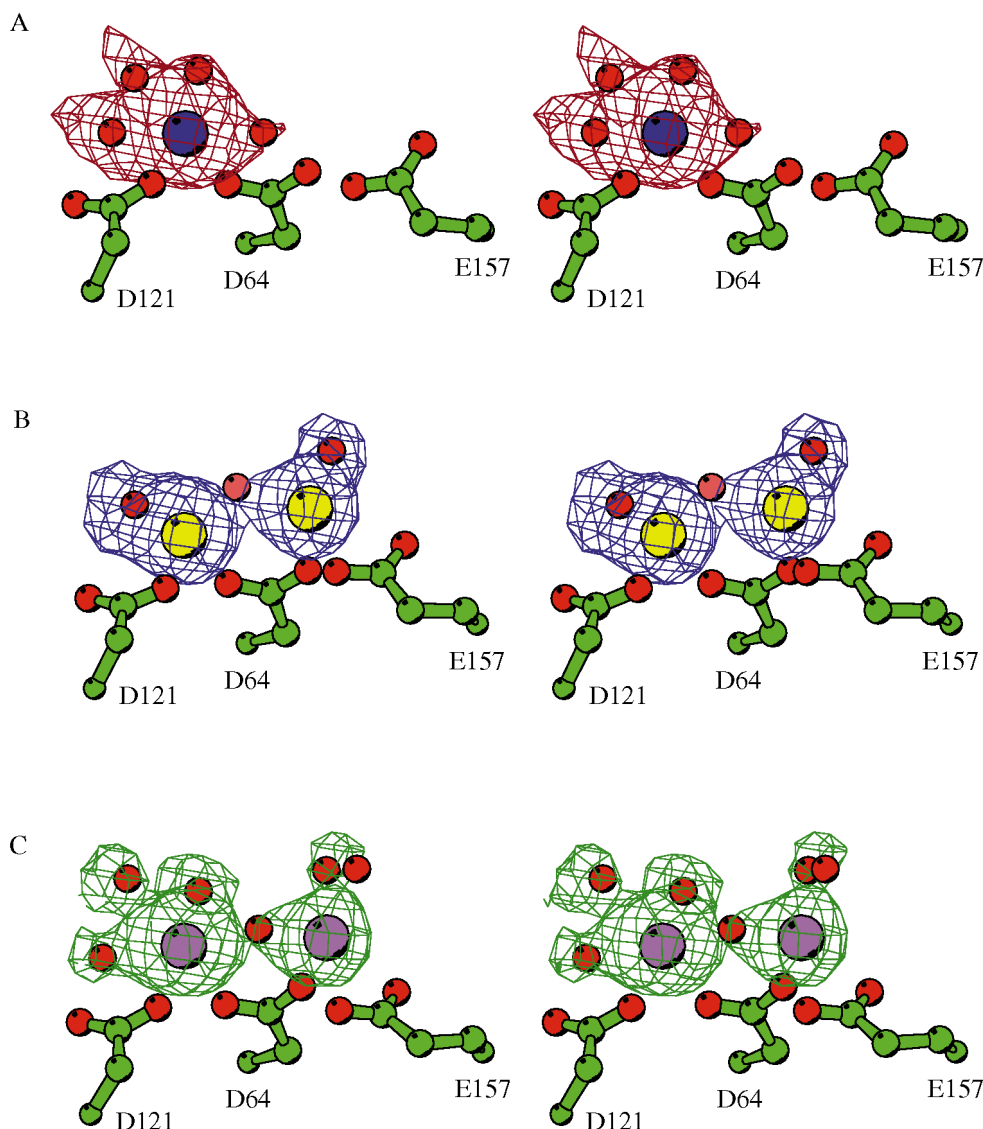


FIG. 1. Stereo views of electron density maps for the complexes of ASV IN with divalent cations. All maps are  $F_o - F_c$  omitmaps, computed with the phases corresponding to the models in which the cation(s) and the neighboring water molecules were removed. The coordinates shown are from the final models. *A*, a map for the complex with 500 mM  $MnCl_2$  calculated at 2.5-Å resolution and contoured at  $2\sigma$  level. The density corresponding to the cluster of an octahedrally coordinated  $Mn^{2+}$  is clear, whereas no density that would be caused by the presence of a second ion can be seen. *B*, a complex with 100 mM  $ZnCl_2$ , calculated at 1.9 Å and contoured at  $3\sigma$  level. The density for both zinc ions is extremely clear, whereas only the bridging water molecule (pink) is out of density. *C*, a complex with 100 mM  $CdCl_2$  with the map calculated at 2.0 Å and contoured at  $2.5\sigma$  level. This figure, as well as Figs. 2 and 6, were generated using MOLSCRIPT (28). This figure only used its modification BOBSCRIPT (R. Esnouf, unpublished). *D*, Asp-; *E*, Glu-.

(10 mM) concentration of  $MnCl_2$ . No additional metal-binding sites were observed, even in 500 mM  $MnCl_2$  (Fig. 1A). A higher apparent affinity for  $Mn^{2+}$  is consistent with observations that ASV IN is approximately 30-fold more active in  $Mn^{2+}$  than  $Mg^{2+}$ .

Crystals soaked in 100 mM  $CaCl_2$  were also found to bind a divalent cation at site I, with interactions between the calcium ion and the active site residues similar to those observed with  $Mg^{2+}$  and  $Mn^{2+}$ . With  $Ca^{2+}$ , coordination is an incomplete octahedron in appearance, a square pyramid with the metal in the center of the square base and three water molecules in the coordination sphere.

***Zn<sup>2+</sup> and Cd<sup>2+</sup> Bind at Multiple Sites in the ASV IN Catalytic Domain***—Unexpectedly, we found that  $Zn^{2+}$  binds in four separate sites on the surface of the isolated catalytic domain of ASV IN (Table I), with partial occupancy observed at a concentration as low as 2 mM and full occupancy of the sites at 100 mM. At the higher concentration of  $Zn^{2+}$ , two of the ions bind in

the catalytic center, one at site I between Asp-64 and Asp-121 and a second, denoted site II, coordinated by Asp-64 and Glu-157 (Fig. 1B). The distance between the zinc cations in the active site is 3.62 Å. Site III (not shown) is in a loop defined by amino acids 92–107, with the ion directly coordinated to His-103, coordinated to His-93 via a water molecule, and liganded with two other water molecules. The fourth zinc ion is bound in the vicinity of the C terminus of the catalytic domain and is coordinated by residues His-198 and Tyr-194 (site IV).

Zinc ions bound at sites III and IV show clear tetrahedral coordination, whereas the cations in sites I and II are coordinated to two oxygens of the carboxylates and one water molecule each. One additional water molecule may complete a tetrahedral coordination of cations in the catalytic center by bridging both zinc ions. This putative water is not seen clearly in the electron density maps; it does, however, appear as a weak peak in  $2F_o - F_{1a}$  maps. During the refinement process, the water molecule located in this position shifts from one edge

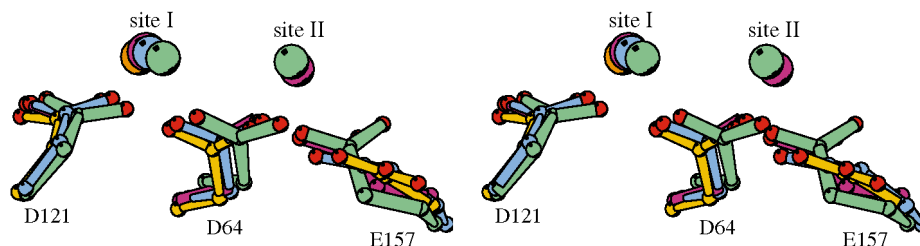


FIG. 2. A stereo view of the active site of ASV IN in the presence of divalent cations. Shown are the superimposed coordinates of the side chains of Asp-64 (*D64*), Asp-121 (*D121*), and Glu-157 (*E157*) as well as the divalent cations. The complexes presented here are with  $\text{Mn}^{2+}$  (yellow),  $\text{Zn}^{2+}$  (green),  $\text{Cd}^{2+}$  (red), and  $\text{Ca}^{2+}$  (blue).

of one  $\text{Zn}^{2+}$  electron density to the other, so it was placed in the final model with null occupancy just to indicate its putative placement. As this water molecule faces bulk solvent, it is not surprising that its position is not well defined. The other water molecules coordinating the zinc ions are found in very clear electron density. With the crystal soaked in 2 mM  $\text{Zn}^{2+}$ , we observed a pattern of metal binding similar to that at 100 mM. In this case, both catalytic binding sites showed less than complete occupancies, with site II lower than site I. Temperature factors are correspondingly higher for site II than for site I. However, the structure with 100 mM  $\text{Zn}^{2+}$  had complete occupancy and relatively low temperature factors for both cations located in the active site.

Two  $\text{Cd}^{2+}$  ions were visible in the catalytic center after soaking in 100 mM  $\text{CdCl}_2$  and were again coordinated to all three carboxylate residues of the essential triad (Fig. 1C). However, there was lower occupancy of site II and higher temperature factor for this ion than for the ion in site I. This is similar to binding observed at the lowest concentration (2 mM) of  $\text{Zn}^{2+}$  and again suggests that the cations in site II may be bound less strongly than those occupying site I. The distance between the cadmium ions in the catalytic center is 4.06 Å (see Fig. 2). The  $\text{Cd}^{2+}$  in site I has an almost perfect octahedral coordination sphere, very similar to the coordination of  $\text{Mn}^{2+}$  and  $\text{Mg}^{2+}$ . The  $\text{Cd}^{2+}$  in site II has deformed octahedral coordination, sharing a water ligand with the first cation. Singularly in this case, both Glu-157 carboxyl oxygens coordinate with this one cation. The most solvent-accessible water molecules liganded to each metal, bound opposite to the Asp-64 ligand, have slightly longer hydrogen bonding distances and higher temperature factors.

The atomic coordinates of the three crucial carboxylic acids are only slightly affected when one or more cations are bound. There is practically no change in the position of the side chain of Asp-64 (mean shift of the atomic positions from their average values, calculated for all structures listed in Table I, is 0.125 Å), a very slight movement of the side chain of Asp-121 (0.187 Å), and a more pronounced difference in location of the side chain of Glu-157 (0.857-Å shift) (Fig. 2). The rotation of the side chain of Glu-157 results in approximately the same difference in carboxylate positions as seen in two different, uncomplexed forms of ASV IN crystallized from different precipitants, polyethylene glycol and ammonium sulfate (11). The minimal deviation in carboxylate positioning upon metal binding is consistent with the observation that even single conservative substitutions in these residues drastically reduced activity of both ASV and HIV-1 IN (8).

**Competition for Cation Binding at the Active Site**—The  $\text{Zn}^{2+}$  structures show the only active sites that are fully occupied with two metal cations at 100 mM concentration (Table I). To determine which cations are preferred by the enzyme, we soaked ASV IN catalytic domain crystals in various concentrations of  $\text{Zn}^{2+}$  plus either  $\text{Mg}^{2+}$  or  $\text{Mn}^{2+}$  salts. In the highest concentration (100 mM for each salt), both structures were essentially identical to the structure with 100 mM  $\text{Zn}^{2+}$  alone.

However, a  $\text{Zn}^{2+}$ ,  $\text{Mn}^{2+}$  structure at 10 mM concentrations of each salt produced a mixed image. The water coordination around the metal occupying active site I appears as a superposition of both  $\text{Zn}^{2+}$  and  $\text{Mn}^{2+}$  structures. We interpreted these maps as a mixture of  $\text{Zn}^{2+}$  and  $\text{Mn}^{2+}$  in site I and only  $\text{Zn}^{2+}$  in site II. As summarized in Table I, the occupancy of zinc cations in sites I and II are refined to be equal. This result may indicate the existence of some cooperativity between the sites, such that if site II is occupied by  $\text{Zn}^{2+}$ , then site I can no longer be occupied by  $\text{Mn}^{2+}$  or  $\text{Mg}^{2+}$ .

**Activity of the ASV IN Catalytic Domain with Various Divalent Cations**—Having observed  $\text{Ca}^{2+}$ ,  $\text{Zn}^{2+}$ , and  $\text{Cd}^{2+}$  occupancy of site I (or I and II) in the active site of the catalytic domain, we asked whether any of these cations could function as cofactors for enzymatic activity of IN. The isolated catalytic core domain of ASV IN displays two metal-dependent activities, a DNA endonuclease “nicking” activity, and a DNA cleavage-ligation “disintegration” activity (11, 20). DNA nicking by the ASV IN catalytic domain is quite efficient and similar in specific activity to that of the full-length protein. Therefore, we first assayed for this nicking activity, which is characterized by preferred cleavage between the C and A of the conserved CA dinucleotide near the viral DNA termini (Fig. 3A, -3). This endonucleolytic activity is distinct from “-2” processing, and its biological relevance is not yet understood. The catalytic core domain was incubated with a short DNA duplex substrate that represents a viral DNA end in the presence of varying concentrations of  $\text{ZnCl}_2$ ,  $\text{ZnSO}_4$ ,  $\text{CaCl}_2$ , and  $\text{CdSO}_4$  as well as the known metal cofactors,  $\text{MgCl}_2$  and  $\text{MnCl}_2$ . Of the new metals tested, only  $\text{Zn}^{2+}$  supported significant activity (comparison not shown). As shown in Fig. 3A, the  $\text{Zn}^{2+}$ -dependent activity exhibits a sharp peak at approximately 2 mM  $\text{ZnSO}_4$ ; similar results were obtained with  $\text{ZnCl}_2$  (data not shown). At this peak, activity is approximately half of that observed with the same concentration of  $\text{MnCl}_2$ . However, significantly less activity is observed at higher  $\text{ZnSO}_4$  concentrations. The optimum concentration of  $\text{MnCl}_2$  is approximately 10 mM, with little change in activity up to 25 mM. The decreased activity at  $\text{ZnSO}_4$  concentrations >2 mM is not due to the anion, as similar results were observed with the chloride and sulfate salts. We conclude that the ASV IN catalytic domain displays significant nicking activity with  $\text{Zn}^{2+}$ , as a cofactor at a concentration in which site I is likely to be fully occupied and site II is likely to be at least partially occupied. Higher concentrations of  $\text{Zn}^{2+}$  are inhibitory. Although  $\text{Mg}^{2+}$  and  $\text{Ca}^{2+}$  could bind to site I and  $\text{Cd}^{2+}$  could bind to sites I and II in the crystal, no nicking activity could be detected in the presence of a broad range of concentrations of these metals (data not shown).

We compared the time-dependent nicking activity of the catalytic domain in the presence of  $\text{Zn}^{2+}$ ,  $\text{Mg}^{2+}$ , and  $\text{Mn}^{2+}$ . The metal concentrations used were 2 mM  $\text{ZnSO}_4$ , 10 mM  $\text{MnCl}_2$  (the optimal concentrations determined above), and 5 mM  $\text{MgCl}_2$ . As illustrated in Fig. 3B, nicking activity is readily detected in the presence of  $\text{ZnSO}_4$ , although the rate and extent

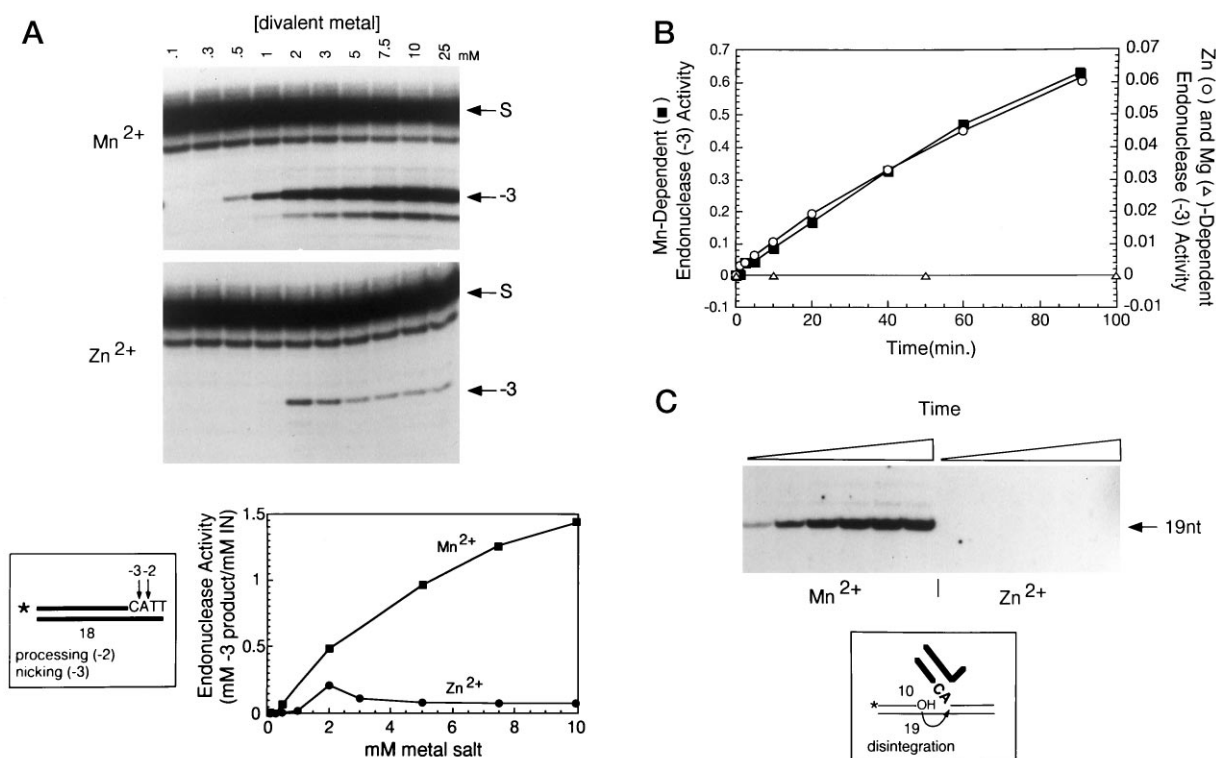


FIG. 3. **Activities of the ASV IN catalytic domain in the presence of Mn<sup>2+</sup>, Mg<sup>2+</sup>, and Zn<sup>2+</sup>.** *A*, the <sup>32</sup>P 18-mer duplex viral DNA substrate (S) was incubated with the ASV IN catalytic domain at the indicated metal concentrations for 150 min. A diagram of the substrate is shown below; the asterisk indicates the 5'-end label. Products were fractionated on 20% sequencing gels. The major product results from cleavage three nucleotides from the 3'-end of the labeled strand (indicated as -3). Quantitation using a Fuji phosphorimager is shown below (averaged from three separate experiments). *B*, time course reaction at fixed divalent cation concentrations: ZnCl<sub>2</sub> (2 mM), MgCl<sub>2</sub> (5 mM), and MnCl<sub>2</sub> (10 mM). Reactions were carried out for the indicated times, and products were fractionated as in panel *A*. Gels were analyzed using a Fuji phosphorimager, and results are displayed graphically. Mn<sup>2+</sup> and Zn<sup>2+</sup> data are the average from three separate experiments. Note the difference in scale for reactions in Mn<sup>2+</sup> versus Zn<sup>2+</sup> and Mg<sup>2+</sup>. *C*, disintegration activity of the catalytic domain. Substrate is shown below. Thick lines indicate viral sequences; the asterisk indicates the 5'-end label. Concerted cleavage-ligation activity results in release of viral sequences and generation of a labeled 19-mer product. The time points were 10, 30, 60, 90, 120, and 150 min. *nt*, nucleotides.

of the reaction are approximately one-tenth that observed with Mn<sup>2+</sup>. However, no activity was detected with MgCl<sub>2</sub>. Thus, at least for the isolated catalytic core domain, we find no activity with the cation presumed to be important *in vivo* but significant activity with Zn<sup>2+</sup> as a cofactor.

The ASV catalytic domain was also assayed for disintegration activity (Fig. 3C), which proceeds at 0.2% of the rate observed with the full-length protein. In the presence of 10 mM MnCl<sub>2</sub>, disintegration is clearly detectable with the catalytic domain, as described previously (20). However, no disintegration activity was observed with 2 mM ZnSO<sub>4</sub>, even after prolonged exposure of the autoradiogram. We conclude that Zn<sup>2+</sup> is unable to support significant disintegration activity of the isolated catalytic domain under these conditions.

**Effects of Metal Combinations on the Nicking Activity of the Catalytic Core**—As noted above, using equimolar (10 mM) amounts of Zn<sup>2+</sup> and Mn<sup>2+</sup>, we observed predominant occupancy of site I by Mn<sup>2+</sup> and exclusive occupancy of site II by Zn<sup>2+</sup>. For comparative activity studies, incubations were carried out using a fixed but suboptimal concentration of Mn<sup>2+</sup> (3 mM) in the presence of increasing concentrations of the divalent metals to be tested, and production of the -3 product was followed as in Fig. 3, *A* and *B*. We observed a slight increase in activity at low or equal concentrations of Mg<sup>2+</sup> relative to Mn<sup>2+</sup> (Fig. 4). As Mg<sup>2+</sup> does not support nicking activity on its own, the significance of this increase is not yet clear. Ca<sup>2+</sup> had no significant effect at the same concentrations, and there was only a slight decrease in activity at higher concentrations of Mg<sup>2+</sup> or Ca<sup>2+</sup>.

In contrast to results with Mg<sup>2+</sup> and Ca<sup>2+</sup>, both ZnCl<sub>2</sub> and

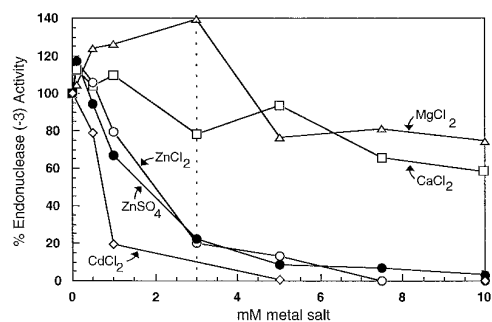


FIG. 4. **Effect of metal combinations on the nicking activity of the ASV IN catalytic domain.** Increasing concentrations of several metal salts (as indicated) were added to reactions containing a suboptimal 3 mM MnCl<sub>2</sub> concentration. Assays were carried out as in Fig. 3A, and the results from phosphorimager analyses are shown graphically. Results are expressed as the percentage activity relative to the MnCl<sub>2</sub> reaction with no added metal salt. The vertical dashed line indicates the point at which the MnCl<sub>2</sub> concentration is equal to that of the second metal salt.

ZnSO<sub>4</sub> showed potent inhibition of Mn<sup>2+</sup>-dependent nicking activity (Fig. 4). At equal concentrations of Zn<sup>2+</sup> and Mn<sup>2+</sup>, the reaction was inhibited approximately 75%. The residual activity observed at this concentration may reflect the Zn<sup>2+</sup>-dependent nicking. Although other interpretations are possible, these results are consistent with inhibition of the Mn<sup>2+</sup>-dependent activity in favor of the Zn<sup>2+</sup>-dependent activity. This potent inhibition by Zn<sup>2+</sup> is also consistent with the apparent high affinity of the isolated catalytic domain for Zn<sup>2+</sup> ions, as exemplified by high occupancy in the crystals even at relatively low

metal concentrations.  $\text{Cd}^{2+}$ , which can also bind to sites I and II but is not a cofactor for nicking by the isolated catalytic core domain, is even a more potent inhibitor than  $\text{Zn}^{2+}$ ; no significant activity was detected with this divalent cation at the higher concentrations (Fig. 4). If we assume that the inhibition reflects the abilities of these metals to bind to the catalytic center, these results suggest a relative affinity corresponding to  $\text{Cd}^{2+}$ ,  $\text{Zn}^{2+} > \text{Mn}^{2+} > \text{Ca}^{2+}$ ,  $\text{Mg}^{2+}$  and is consistent with the results shown in Table I.

**$\text{Zn}^{2+}$  Can Serve as a Cofactor for the Processing Activity of Full-length ASV IN**—We next asked if  $\text{Zn}^{2+}$  or the other previously untested divalent metals could function as a cofactor for the processing and joining activities of full-length ASV IN. Our initial survey revealed no significant activity with full-length IN in a range of concentrations of  $\text{Ca}^{2+}$  or  $\text{Cd}^{2+}$  (data not shown).  $\text{Zn}^{2+}$  did support activity with an optimal concentration of 2 mM (not shown). We then compared the activities in the presence of 2 mM  $\text{ZnSO}_4$  or 10 mM  $\text{MgCl}_2$  (the optimal concentration, data not shown). As illustrated in Fig. 5A, the full-length IN showed significant processing activity ( $-2$  nicking) in the presence of  $\text{Zn}^{2+}$ ; this activity is slightly reduced compared with that observed with  $\text{Mg}^{2+}$ , but both are approximately 10-fold lower than that observed with  $\text{Mn}^{2+}$  as the cofactor (not shown). Joining activity can be detected as insertion events into the viral DNA substrate, which produces a ladder of products that is longer than the substrate (Fig. 5C). As expected, joining activity is readily detected in the presence of  $\text{Mg}^{2+}$ ; however, no significant joining activity was observed with  $\text{Zn}^{2+}$ .

**The N-terminal Domain Is Not Required for Zinc-dependent Processing Activity**—We previously showed that IN-(39–286), a non-fused ASV IN derivative lacking the N-terminal zinc binding domain, displays near wild type levels of processing and joining activity in the presence of  $\text{Mn}^{2+}$  (19). As shown in Fig. 5 (B and D), the processing and joining activities of IN-(39–286) in  $\text{Mg}^{2+}$  are also similar to that of the full-length IN. Near wild type processing activity can also be detected with IN-(39–286) in the presence of  $\text{Zn}^{2+}$  (Fig. 5B). From these results, we conclude that the N-terminal domain is not required for the zinc-dependent processing activity. However, quantitation by phosphoimaging of panels A and B of Fig. 5 indicates that deletion of the N-terminal domain does cause some ( $\sim 70\%$ ) reduction in apparent rates in the presence of  $\text{Zn}^{2+}$ . This suggests two roles for  $\text{Zn}^{2+}$  in these experiments: a structural role in stabilizing the N-terminal domain, which, as our comparison indicates, is required for optimal activity, and a catalytic role, as the only available cation cofactor.

We also assayed the IN-(39–286) protein for disintegration activity. As shown in Fig. 5E, this activity was quite robust in  $\text{Mn}^{2+}$ , as shown previously. Activity in  $\text{Mg}^{2+}$  was readily detectable, whereas activity was detected in  $\text{Zn}^{2+}$  only after prolonged exposure of the gel. Quantitation by phosphoimaging indicated that the rate of disintegration in  $\text{Zn}^{2+}$  was reduced by approximately 3 logarithms compared with  $\text{Mn}^{2+}$  and 2 logarithms compared with  $\text{Mg}^{2+}$  (data not shown). From these results, we conclude that  $\text{Zn}^{2+}$  cannot support significant disintegration activity of IN-(39–286). Interestingly, as with the full-length protein,  $\text{Zn}^{2+}$  also fails to support significant joining activity by IN-(39–286) (Fig. 5D).

#### DISCUSSION

Many enzymes active in the nucleic acid metabolism have an absolute requirement for divalent cations. However, details of the arrangements of such cations have been reported in only a few of the published structures. In the case of ASV IN, we previously identified binding of  $\text{Mn}^{2+}$  and  $\text{Mg}^{2+}$  to a single site between Asp-64 and Asp-121 (site I). Here we report the binding of two zinc ions and two cadmium ions to sites I and II. Site

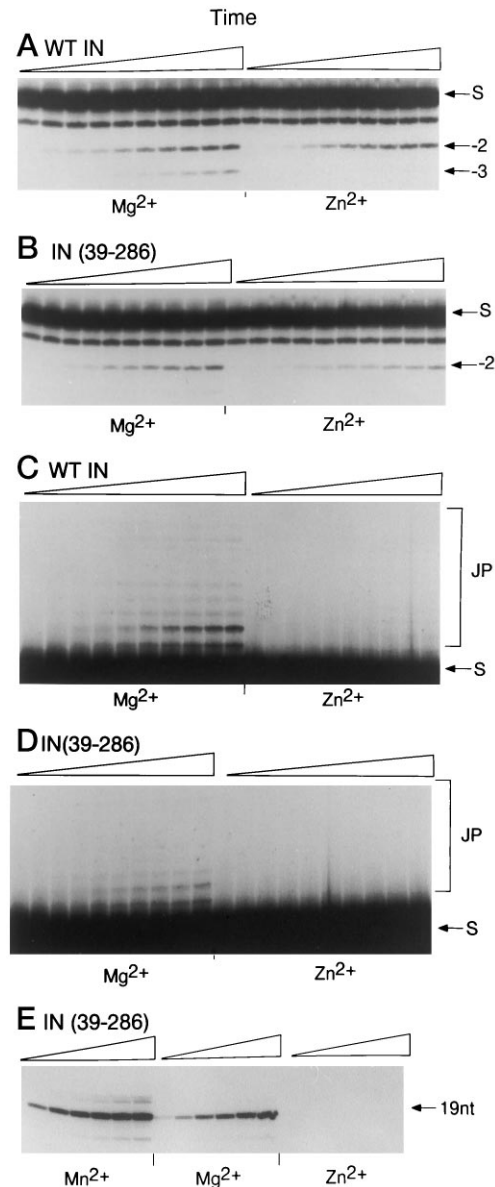


**FIG. 5. Processing, joining, and disintegration activities of full-length IN (WT IN) and a zinc finger domain deletion mutant (IN-(39–286)) in the presence of  $\text{Mg}^{2+}$  and  $\text{Zn}^{2+}$ .** Assays were carried out as described in Fig. 3A. Processing activity is characterized by 3' cleavage of the conserved CA two nucleotides from the 3'-end of the labeled strand ( $-2$  site). Joining activity is characterized by the appearance of joined products (JP) longer than substrate length. Reactions were carried out in 2 mM  $\text{ZnSO}_4$  and 10 mM  $\text{MgCl}_2$  from 1 to 75 min. Panels C and D show a prolonged exposure of the region above the substrate bands in panels A and B in order to display joined products. Panel E shows disintegration activity as described in Fig. 3C. The time points were 10, 30, 60, 90, 120, and 150 min. S,  $^{32}\text{P}$  18-mer duplex viral DNA substrate; WT, wild type; nt, nucleotides.

II ligands are Asp-64 and Glu-157, suggesting a role for this third member of the invariant triad in the D,D(35)E motif. Two more  $\text{Zn}^{2+}$  cations are located away from the active site of the enzyme. As it is not yet known if these sites can be occupied in the full-length protein, the significance of this binding cannot be evaluated. It is possible that metal ions bound to one or both of these sites could play a role in structural stabilization and/or activity control, as reported for other enzymes (21).

It is not certain why the complexes with different divalent cations show differential occupancy of site II. Each of the two sites contains two direct links to the protein through carboxyl oxygens, but in all structures of the isolated catalytic domain,

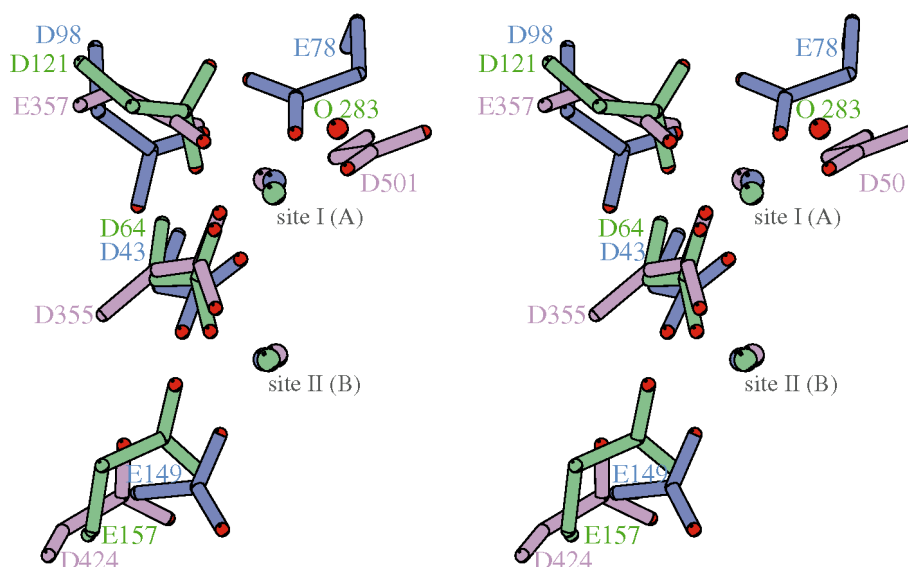


FIG. 6. The environment of  $Mg^{2+}$  and  $Zn^{2+}$  divalent cations in the active site of polynucleotidyltransferases. The residues forming the D,D(35)E motif in the active site of ASV IN (green) are compared with the equivalent sites of HIV-1 RNase H (blue) as well as of the exonuclease domain of the Klenow fragment of DNA I polymerase I (pink). One of the water molecules present in site I of ASV IN is found in a position occupied by carboxylate oxygens (O) in the other two structures. D, Asp; E, Glu.

the temperature factors for Glu-157 are considerably higher than for the two aspartates in the active site, indicating higher mobility of that side chain. This may cause more difficulty for binding of the octahedrally coordinated  $Mg^{2+}$ ,  $Mn^{2+}$ , or  $Ca^{2+}$  than the tetrahedrally coordinated  $Zn^{2+}$ , which has less stringent requirements for the geometry of its binding site and a lower preferred coordination number (22). This does not explain why the octahedrally coordinated  $Cd^{2+}$  would bind in site II, but we note that this ion is able to utilize both oxygens of Glu-157 for its binding, and this might enhance its stability.

The structural features of zinc ions in the active site agree well with the description of other co-catalytic sites in multi- $Zn^{2+}$  or  $Mg^{2+}$  plus  $Zn^{2+}$  enzymes discussed by Vallee and Auld (23). As is commonly the case, both ions are close to each other (the distance is 3.62 Å in the high occupancy structure), and they are bridged by the carboxylate group of an aspartic acid (e.g. Asp-64). Similar arrangements have been reported in the past for other enzymes, such as phospholipase C (24) and nuclease P1 (25). In common with these structures, there is also indication of a shared water molecule bridging the two cations, although this putative water is not well ordered in ASV IN.

**Active Sites of Polynucleotidyltransferases Bear Considerable Similarity**—In the absence of a bound DNA substrate, the current structural data do not allow us to propose any specific model concerning metal binding to site II and the mechanism by which hydrolysis or nucleotidyl transfer occurs with ASV IN. Yang and Steitz (14) have noted the similarity of the cluster of acidic residues forming the active sites of enzymes in the structural superfamily to which integrase belongs, and more detailed comparisons of metal complexes of some of the members of this family were presented by Bujacz *et al.* (12). The binding of two metal ions in the ASV IN active site reported here invites comparison with the 3'-5' exonuclease domain of the *E. coli* DNA polymerase I (Klenow fragment) in which two metals are proposed to cooperate to activate an attacking hydroxide and stabilize a pentacoordinate DNA phosphate transition state in the active site (14, 15). In Fig. 6, we compare metal complexes of the active sites of ASV IN, HIV-1 reverse transcriptase RNase H, and the exonuclease domain of the Klenow fragment of DNA polymerase I (15). Despite significant differences in topologies of the three proteins, the similarity in positions of both divalent cations and the coordinating carboxyl-

ates is apparent. In this alignment, site I of ASV IN is superimposed on site A of the Klenow fragment, both of which have been shown to have similar metal binding properties in terms of occupancy and metal ligand geometry. Alignment of site I of ASV IN with site B of the exonuclease domain does not yield as good a superposition of the coordinating residues.

Some differences between these enzymes are also clear. When a mixture of divalent cations is present, site A in the Klenow fragment is occupied by a  $Zn^{2+}$  ion, whereas site B is occupied by  $Mg^{2+}$ , with clear differences in the octahedral *versus* tetrahedral coordination. This is not the case for integrase, because  $Zn^{2+}$  clearly is preferred in both sites under higher metal concentrations, both with tetrahedral coordination. As there are only two carboxylate oxygens binding each ion, there are no geometric constraints that favor or necessitate one type of coordination. These differences may be due to the absence of coordinating ligands contributed by other portions of ASV IN or the DNA substrate. For both integrase and exonuclease, the concentration of  $Zn^{2+}$  necessary to observe binding is more than an order of magnitude lower than that for  $Mg^{2+}$ . Active sites that contain more than one type of divalent cation are observed in other  $Zn^{2+}$ -containing enzymes that act upon phosphate esters. The second metal ion is often  $Mg^{2+}$  as, for example, in phospholipase C or alkaline phosphatase (24, 25).

It is important to note that active site configurations different from those shown in Fig. 6 are observed for other enzymes with DNA-processing or polymerizing activity. Two divalent cations are reported in one of the structures of rat polymerase  $\beta$  (26), separated by about 3.7 Å and also coordinated by three acidic residues, yet we could obtain no convincing superposition on the active site of integrase. Even more different is the active site of phage T4 RNase H (27) where the two  $Mg^{2+}$  ions are 6.3 Å apart, with one of them coordinated by only a single carboxylate oxygen and five water molecules, whereas the other is surrounded by six water molecules and does not make direct contacts with any protein atom. These examples show the limits of the comparisons and are a caveat against drawing conclusions that might be too far-reaching.

**Biochemical Activity of Divalent Cations**—Our biochemical analyses show that although  $Zn^{2+}$  is less effective than  $Mn^{2+}$ , it can serve as a cofactor for nicking activity of the isolated catalytic core domain of ASV IN, whereas there is no detectable

activity with  $Mg^{2+}$ ,  $Ca^{2+}$ , or  $Cd^{2+}$ . Comparisons of nicking activities in mixtures of  $Mn^{2+}$  and the other cations suggest that both  $Zn^{2+}$  and  $Cd^{2+}$  bind with higher affinity than  $Mn^{2+}$  and that  $Mg^{2+}$  and  $Ca^{2+}$  bind with lower affinity. This is consistent with the occupancies of these metals observed in our structural analyses of the catalytic domain. We also observed a sharp peak for the optimal concentration of  $Zn^{2+}$  at 2 mM; higher concentrations were inhibitory. The reason for this decreased activity at higher  $Zn^{2+}$  concentrations is not yet apparent. However, the most striking result from these studies was the observation that  $Zn^{2+}$  supported the endonuclease activity of the catalytic domain, whereas  $Mg^{2+}$ , the presumed physiologically relevant cation, did not. This observation prompted us to ask whether  $Zn^{2+}$  or any of the other catalytic domain binding cations could serve as cofactors for processing and joining by the full-length enzyme.

As ASV IN can perform both processing and joining *in vitro*, in the absence of the N-terminal domain it is possible to separate the presumed structural role of  $Zn^{2+}$  bound to the N-terminal domain from a catalytic role. We found that both full-length ASV IN and IN-(39–286), which lacks the N-terminal  $Zn^{2+}$  binding motif, display both  $Mg^{2+}$ - and  $Zn^{2+}$ -dependent endonucleolytic processing activity. The  $Mg^{2+}$ -dependent activity is somewhat higher with the full-length protein than with IN-(39–286), indicating that the N-terminal domain is required for optimal activity. Most importantly, both full-length and IN-(39–286) showed  $Zn^{2+}$ -dependent processing activity almost equal to that observed with  $Mg^{2+}$ . Other investigators have reported that the addition of  $Zn^{2+}$  can enhance the  $Mg^{2+}$ -dependent activity of HIV-1 IN (6, 7). However, in their studies, stimulation was shown to be mediated by the N-terminal zinc binding domain. Thus, ours is the first report that  $Zn^{2+}$  can also act as a cofactor for catalysis by a retroviral integrase.

In contrast to results with processing, we could detect no joining activity by either full-length ASV IN or IN-(39–286) in the presence of  $Zn^{2+}$ . We also observed that  $Zn^{2+}$  fails to support significant disintegration activity by either the catalytic core domain or IN-(39–286). Thus, the two reactions in which the nucleophile is derived from a DNA moiety and contact with "target" DNA sequences is required (*i.e.* joining and disintegration) are greatly impaired with  $Zn^{2+}$  as a cofactor. As the same triad of acidic amino acids in the catalytic center is essential for both processing and joining in the presence of  $Mn^{2+}$  and  $Mg^{2+}$  and these steps employ similar chemistry, there is no obvious explanation for this difference. It is possible that the lower preferred coordinating number of  $Zn^{2+}$  compared with  $Mn^{2+}$  or  $Mg^{2+}$  disfavors interactions with target

DNAs or links to the protein that affect target DNA binding. Further structural analyses should help us to understand the basis for these distinct metal preferences. Lastly, the fact that  $Zn^{2+}$  binds tightly to the active site but can only support one step in integration may be relevant to the design of active site inhibitors of retroviral integrases.

*Acknowledgments*—We acknowledge the participation of M. Jaskólski in the initial stages of this project. We thank D. Matthews, L. Beese, and R. Almassy for the unpublished coordinates of proteins and G. Palm for the computer program for multiple alignment of the coordinate sets.

#### REFERENCES

- Katz, R. A., and Skalka, A. M. (1994) *Annu. Rev. Biochem.* **63**, 133–173
- Goff, S. P. (1992) *Annu. Rev. Genet.* **26**, 527–544
- Vink, C., Groeneger, O. A. M., and Plasterk, R. H. (1993) *Nucleic Acids Res.* **21**, 1419–1425
- Andrake, M. D., and Skalka, A. M. (1996) *J. Biol. Chem.* **271**, 19633–19636
- Lee, S. P., Xiao, J., Knutson, J. R., Lewis, M. S., and Han, M. K. (1997) *Biochemistry* **36**, 173–180
- Lee, S. P., and Han, M. K. (1996) *Biochemistry* **35**, 3837–3844
- Zheng, R., Jenkins, T. M., and Craigie, R. (1996) *Proc. Natl. Acad. Sci. U. S. A.* **93**, 13639–13664
- Kulkosky, J., Jones, K. S., Katz, R. A., Mack, J. P., and Skalka, A. M. (1992) *Mol. Cell. Biol.* **12**, 2331–2338
- Dyda, F., Hickman, A. B., Jenkins, T. M., Engelman, A., Craigie, R., and Davies, D. R. (1994) *Science* **266**, 1981–1986
- Bujacz, G., Alexandratos, J., Zhou-Liu, Q., Clement-Mella, C., and Wlodawer, A. (1996) *FEBS Lett.* **398**, 175–178
- Bujacz, G., Jaskólski, M., Alexandratos, J., Wlodawer, A., Merkel, G., Katz, R. A., and Skalka, A. M. (1995) *J. Mol. Biol.* **253**, 333–346
- Bujacz, G., Jaskólski, M., Alexandratos, J., Wlodawer, A., Merkel, G., Katz, R. A., and Skalka, A. M. (1996) *Structure (Lond.)* **4**, 89–96
- Davies, J. F., II, Hostomska, Z., Hostomsky, Z., Jordan, S. R., and Matthews, D. A. (1991) *Science* **252**, 88–95
- Yang, W., and Steitz, T. A. (1995) *Structure (Lond.)* **3**, 131–134
- Beese, L. S., and Steitz, T. A. (1991) *EMBO J.* **10**, 25–33
- Rice, P., Craigie, R., and Davies, D. R. (1996) *Curr. Opin. Struct. Biol.* **6**, 78–83
- Otwinowski, Z. (1992) *An Oscillation Data Processing Suite for Macromolecular Crystallography*, Version 1.6.2, Yale University Press, New Haven, CT
- Hendrickson, W. A. (1985) *Methods Enzymol.* **115**, 252–270
- Katz, R. A., Merkel, G., and Skalka, A. M. (1996) *Virology* **217**, 178–190
- Kulkosky, J., Katz, R. A., Merkel, G., and Skalka, A. M. (1995) *Virology* **206**, 448–456
- Kim, J. L., Morgenstern, K. A., Lin, C., Fox, T., Dwyer, M. D., Landro, J. A., Chambers, S. P., Markland, W., Lepre, C. A., O'Malley, E. T., Harbeson, S. L., Rice, C. M., Murcko, M. A., Caron, P. R., and Thomson, J. A. (1996) *Cell* **87**, 343–355
- Bock, C. W., Katz, A. K., and Glusker, J. P. (1995) *J. Am. Chem. Soc.* **117**, 3754–3765
- Vallee, B. L., and Auld, D. S. (1993) *Biochemistry* **32**, 6493–6500
- Hough, E., Hansen, L. K., Birknes, B., Jynge, K., Hansen, S., Hordvik, A., Little, C., Dodson, E., and Derewenda, Z. (1989) *Nature* **338**, 357–360
- Volbeda, A., Lahm, A., Sakiyama, F., and Suck, D. (1991) *EMBO J.* **10**, 1607–1618
- Davies, J. F., II, Almassy, R. J., Hostomska, Z., Ferre, R. A., and Hostomsky, Z. (1994) *Cell* **76**, 1123–1133
- Mueser, T. C., Nossal, N. G., and Hyde, C. C. (1996) *Cell* **85**, 1101–1112
- Kraulis, P. J. (1991) *J. Appl. Crystallogr.* **24**, 946–950